



Colored cotton fabric with hydrophobicity prepared by monodispersed cationic colored polymer nanospheres

Yi Yang¹ · Min Li¹ · Shaohai Fu¹

Received: 11 April 2021 / Revised: 30 May 2021 / Accepted: 4 June 2021 / Published online: 19 June 2021
© The Author(s), under exclusive licence to Springer-Verlag GmbH Germany, part of Springer Nature 2021

Abstract

Colored polymer nanospheres have high light absorption, reflection, and color properties, which can be widely used as the colorants in inks, textiles, and paints. In this paper, the monodispersed cationic colored polymer nanospheres (RCCM, YCCM, and BCCM) with the three-primary colors were fabricated by emulsion polymerization using polymerizable dyes (AHAQ, AAQBC, and AHMAQ) and styrene (St) as the monomers. The polymerizable dyes were successfully synthesized, and their chemical structures were characterized by ¹H-NMR, FT-IR, and elemental analysis. The diameters and zeta potential of RCCM, YCCM, and BCCM were 65 nm, 68 nm, 69 nm, and +42.8 mV, +45.3 mV, and +50.6 mV, respectively. Importantly, the prepared nanospheres exhibited high dispersion stability due to their high zeta potential. Then the RCCM, YCCM, and BCCM were applied to CMC-treated cotton fabric printing without any extra additives. The printed fabrics exhibited a certain hydrophobicity with the contact angles (CA) of 125°, 128°, and 123°. The testing of hand feel indicated that the hand feel of printed fabrics changed slightly as compared with cotton fabrics. And the color fastness of all printed fabrics was good enough for practical applications.

Keywords Polymerizable dyes · Nanospheres · Printing · Cotton fabric · Hydrophobicity

Introduction

Cotton is the most widely used cellulosic raw material in the textile industry owing to its outstanding properties such as high permeability, renewability, biodegradability, and high strength [1–5]. The coloring of textiles can improve wearability of textiles. For cotton fabric, reactive dyes have become the most favorable dyes for cotton fabrics because of their brilliant colors, excellent washing fastness, low price, and reactivity to cotton fabrics [6, 7]. However, the salts, such as NaCl and Na₂SO₄, must be added to the dye bath for decreasing the electrostatic repulsion between reactive dyes and cotton fabric and increasing the exhaustion of the dyes [1, 8, 9]. Furthermore, although the addition of alkali can

accelerate the formation of covalent bonds between reactive dyes and cotton fabric and promote the fixation, it also can cause the hydrolysis of dyes and the lower utilization (50–70%) of dyes [10, 11]. The salts and hydrolyzed dyes are retained in the waste liquid after dyeing contains, which causes serious water pollution and increases dyeing cost by 10% [7, 12, 13]. It is a great challenge for researchers to prepare a new colorant for dyeing cotton fabrics and solving environmental pollution.

Colored polymer colorants have aroused attention in recent years due to their large specific surface areas, uniform particle sizes, controllable colors, and unique optical properties [14–18]. Combining colorant components and polymer components through physical interaction is a method for preparing colored polymer colorants. For example, Fang and Ren [19] utilized the disperse dyeing method to prepare the colored nanospheres, and these novel colored nanospheres exhibited uniform diameter and brilliant color, which have great potential application in the textile industry. Furthermore, Fang et al. also [20] reported a method of absorption reactive dyes onto the cationic polymer microsphere surface to prepare dye/copolymer nanospheres, and it was further applied on dyeing of cotton fabric. However, because of the

✉ Min Li
minmin0421@163.com

✉ Shaohai Fu
shaohaifu@hotmail.com

¹ Jiangsu Engineering Research Center For Digital Textile Inkjet Printing, Ministry of Education, Key Laboratory of Eco-Textile, Jiangnan University, Wuxi 214122, Jiangsu, China

poor interaction between dyes and polymers, the desorption or leakage of dyes occurred. Building the chemical bonds between colorants and polymer is an effective method for fabricating colored polymer colorants. For example, Yang et al. [21] used the covalent bonds to graft reactive dye on the surface of nanospheres, and it was further applied to binder-free pigment printing. The results indicated that the printed fabric had a softer hand feel and better color fastness as compared with conventional pigment printing with a large number of binders.

Herein, we prepared monodispersed cationic colored polymer nanospheres with different colors, which can be used as the colorants to print the cotton fabric. Firstly, polymerizable dyes with three colors of red, yellow, and blue (AHAQ, AAQBC, and AHMAQ) were synthesized and their chemical structures were characterized by ¹H-NMR, FT-IR, and elemental analysis. Subsequently, monodispersed cationic colored polymer nanospheres (RCCM, YCCM, and BCCM) were prepared through emulsion polymerization by St and polymerizable dyes. The size distribution, zeta potential, and morphology were measured by DLS and TEM. The dispersion stability of RCCM, YCCM, and BCCM was also tested. Finally, RCCM, YCCM, and BCCM were applied to print CMC-treated cotton fabric without any additives. The hydrophobicity, color performance, hand feel, and color fastness of printed cotton fabrics were studied.

Experimental section

Materials

Cotton fabric (140 g/m²) was purchased from Xinfeng Printing and Dyeing Co., Ltd. (Huzhou, China). 1-Nitroanthraquinone (AQ), 1-aminoanthraquinone (NAQ), and 2,2'-azobis[2-methylpropionamide]-dihydrochloride (AIBA) were obtained from the J&K Scientific Co., Ltd. (Shanghai, China). 1-Bromo-4-(methylamino) anthraquinone (AHQ) was purchased from Zhengzhou Alpha Chemical Co., Ltd. (Zhengzhou, China). Carboxymethyl cellulose (CMC, 99.8%, Mn = 25,000) was obtained from Aladdin Industrial Co., Ltd. (Shanghai, China). Cationic emulsifier (CTE-31770) was obtained from Zhengzhou Yihe Fine Chemicals Co., Ltd. (Zhengzhou, China). 1,6-Hexylenediamine, terephthaloyl chloride, 2-hydroxyethyl acrylate, styrene (St), ammonium persulfate (APS), polyoxyethylene octylphenol ether-10 (OP-10), sodium lauryl sulfate (SDS), and dimethylsulfoxide (DMSO) were obtained from Sinopharm Chemical Reagent Co., Ltd. (Shanghai, China). Ammonium polyacrylate thickener (DM-5229) was purchased from DYMATIC Chemicals Co., Ltd. (Shanghai, China).

Synthesis of 1-(6-acrylamidohexylamino) anthraquinone

Synthesis of 1-(6-aminohexylamino) anthraquinone (AMAQ). A total of 4.64 g (40 mmol) of 1,6-diaminohexane was stirred to a mixture containing dimethoxyethane (50 mL), 1-nitroanthraquinone (2.53 g, 10 mmol), and Na₂CO₃ (1.06 g, 10 mmol), and refluxed at 85 °C for 2 h. The above mixture was cooled at room temperature and poured into an aqueous NaOH solution (0.2 wt%). The solid precipitate was filtered and washed with deionized water three times. After evaporation of water at reduced pressure, the product (AMAQ) was purified by recrystallization from ethyl acetate to obtain the dark red solid.

Synthesis of 1-(6-acrylamidohexylamino) anthraquinone (AHAQ). AMAQ (2.58 g, 8 mmol) and triethylamine (1.2 g, 12 mmol) were dissolved in dichloromethane (40 mL) and transferred into a three-necked flask in an ice bath. A total of 0.905 g of acryloyl chloride (10 mmol), dissolved in dichloromethane (10 mL), was slowly added to the above solution over 15 min. The endpoint of the reaction was monitored by thin-layer chromatography (TLC) using a mixture of dichloromethane/ethyl acetate (3:1 v/v) as the mobile phase. After removal of the residual developing solvents, the AHAQ was prepared.

Synthesis of 2-acroyloxyethyl-4-(anthraquinone-1-ylcarbamoyl) benzoate

Synthesis of 4-(anthraquinone-1-ylcarbamoyl) benzoyl chloride (AABC). Terephthaloyl chloride (10.15 g, 50 mmol), 1-aminoanthraquinone (2.23 g, 10 mmol) were added into a stand-up flask containing toluene (80 mL). The above mixture was stirred and refluxed at 115 °C for 3 h. It was cooled at room temperature and then poured into n-hexane (400 mL). The bright yellow product (AABC) was obtained after filtering and washing with n-hexane three times.

Synthesis of 2-acroyloxyethyl-4-(anthraquinone-1-ylcarbamoyl) benzoate (AAQCB). AABC (3.12 g, 8 mmol), triethylamine (1.2 g, 12 mmol), and 2-hydroxyethyl acrylate (2.78 g, 24 mmol) were dissolved in dichloromethane (40 mL) and stirred at room temperature for 4 h. The above mixture was poured into n-hexane (400 mL). The product was filtered and purified by thin-layer chromatography (TLC) using a mixture of dichloromethane/ethyl acetate (3:1 v/v) as the mobile phase. After removal of the residual developing solvents, the AAQCB was obtained.

Synthesis of 1-(6-acrylamidohexylamino)-4-(methylamino) anthraquinone

Synthesis of 1-(6-aminohexylamino)-4-(methylamino) anthraquinone (AHMQ). A total of 9.28 g (80 mmol) of

1,6-diaminohexane was added to a suspension containing DMSO (80 mL), 1-bromo-4-(methylamino) anthraquinone (6.32 g, 20 mmol), anhydrous copper acetate (3.66 g, 20 mmol), and potassium acetate (1.96 g, 20 mmol), and the reaction was carried out with stirring at 90 °C for 2 h. The mixture was cooled to room temperature and then poured into an aqueous NaOH solution (0.1 wt%). The precipitate was filtered and washed with deionized water three times. After evaporation of water at reduced pressure, the dark blue solid (AHMQ) was purified by recrystallization from ethyl acetate.

Syntheses of 1-(6-acrylamidohexylamino)-4-(methylamino) anthraquinone (AHMAQ). AHMQ (3.51 g, 10 mmol), and triethylamine (1.5 g, 15 mmol) were dissolved in dichloromethane (40 mL) and transferred into a three-necked flask in an ice bath. A total of 1.09 g of acryloyl chloride (12 mmol), dissolved in dichloromethane (10 mL), was slowly added to the above solution over 15 min. The endpoint of the reaction was monitored by thin-layer chromatography (TLC) using a mixture of dichloromethane/ethyl acetate (3:1 v/v) as the mobile phase. AHMAQ was obtained by removing the residual developing solvents.

Preparation of cationic colored polymer nanospheres and their dispersion

Cationic colored polymer nanospheres were prepared by emulsion polymerization. The specific recipe is shown in Table 1. Firstly, the cationic emulsifier CTE-31770 was dissolved in deionized water (95 mL) to obtain an aqueous phase. Then the polymerizable dyes (AHAQ, AAQCB, and AHMAQ) were dissolved in the monomer of St to form the oil phases, respectively. The oil phase was mixed with the aqueous phase under ultrasonic stirring at 300 rpm for 15 min. Then, the above mixture was transferred to a 250-mL four-neck round bottom glass flask with N₂ and a mechanical stirrer. After the temperature was raised to 80 °C, 5 mL of

Table 1 Recipes for preparation of cationic colored polymer nanospheres

Ingredients	RCCM	YCCM	BCCM
AHAQ (g)	Variable amount ^a	—	—
AAQCB (g)	—	Variable amount ^a	—
AHMAQ (g)	—	—	Variable amount ^a
St (g)	10	10	10
CTE-31770 (g)	2	2	2
AIBA (g)	0.15	0.15	0.15
Water (g)	100	100	100

^a0–1.5 wt% based on total monomers

AIBA solution was put into it within 5 min, then reaction at 80 °C for 24 h. Finally, the red cationic colored polymer nanospheres (RCCM) dispersion, blue cationic colored polymer nanospheres (BCCM) dispersion, and yellow cationic colored polymer nanospheres (YCCM) dispersion were obtained after filtration of the sediment. RCCM dispersion, BCCM dispersion, and YCCM dispersion were freeze-dried to obtain RCCM, BCCM, and YCCM nanospheres powders.

Printing of cotton fabric

CMC treatment of cotton fabric The cotton fabrics were modified with CMC according to the previously reported methods [22, 23]. The cotton fabrics were washed with a 0.1-mol/L HCl solution for 30 min to remove the metal ions and convert ionizable groups on the fibers into their acid form. Then the cotton fabrics were washed with deionized water until the conductivity of washed water reached 2 μS/cm. The ionizable groups were changed into their Na-form by washing with 1 mmol/L NaHCO₃ at pH = 9 (adjusted with 0.1 mol/L NaOH) and followed by washing with deionized water until the conductivity reached 2 μS/cm. Finally, the preprocessed cotton fabrics were immersed into a solution of 20 mg CMC per gram fibers in 0.05 mol/L CaCl₂ at pH = 7–8 and 80 °C for 2 h. The treated cotton fabrics were washed with deionized water until the conductivity of the washed water was 2 μS/cm.

Printing process The RCCM, YCCM, and BCCM printed fabrics were obtained by screen printing. The recipe for printing paste is shown in Table 2.

Characterization

The UV–vis absorption spectra of samples were recorded with a UV–vis spectroscopy (UV-2450, Shimadzu, Japan). The FT-IR spectra of the samples were obtained with a spectrometer (NICOLETS50, Nicolet Instrument Corporation, USA). The structures of prepared polymerizable dyes were characterized by a 400-MHz digital spectrometer (AVANCE III, Bruker AXS GmbH, Germany) using CDCl₃ and DMSO as the solvents and TMS as the internal standard. Element analysis for C, H, N, and O was performed

Table 2 The recipe for printing paste

Components	Printed fabrics
RCCM/YCCM/ BCCM (g)	0.5
DM-5229 (g)	3
Water (g)	46.5
Totally (g)	50

on a Vario MACRO cube (Elementar Co., Ltd, Germany). Thermogravimetric analysis (TGA) was performed under nitrogen conditions using a TG apparatus (TGA/SDTA851e, Mettler Toledo Instrument Co., Ltd, Switzerland) with a 15 °C/min ramp between 30 and 800 °C. Differential scanning calorimetry (DSC) was performed using a differential scanning calorimeter (TQ-200, TA Instruments, USA). The crystalline structure of samples was analyzed by XRD (D2 PHASER, Bruker AXS Co., Ltd, Germany) equipped with Cu K radiation (40 kV and 200 mA) in a 2θ between 5 and 90°. The mean particle size of samples was measured by dynamic light scattering (DLS) with Malvern Particle Size Analyzer (Nano-ZS90, Malvern Instruments Co., Ltd., England) at 25 °C. Each sample was measured three times and reported as an average value. The surface morphologies of cotton fabrics were observed by scanning electron microscope (SU1510, Hitachi, Japan) at an accelerating voltage of 5.0 kV. The morphology of samples was observed by the transmission electron microscope (TEM) (H-7000, Hitachi, Japan). The contact angle (CA) of static water droplets (5 μL) was measured using the contact angle meter equipped with a CCD camera (Ramehart Instrument Co., Ltd.). Fastness properties to washing and rubbing were evaluated according to the respective international standards: ISO 105-C06 (A1S): 2010 and ISO 105-X12 (2016). The color strength (K/S) and color difference (ΔE) of the printed fabric were determined by Datacolor SP600 + spectrophotometer (Datacolor, Switzerland). The cotton fabrics were cut to a circle with an area of 100 cm², and the weight and thickness of the fabrics were tested. The fabrics were placed at 20 °C and 65% RH on a sample rack for at least 4 h. Finally, the hand feel of cotton fabrics was measured by a PhabrOmeter® model 3 testers (Nu Cybertek, Inc., USA) according to the AATCC Test Method 202–2014. The thermal stability (S_T), centrifugal stability (S_C) and storage stability (S_{ST}) were evaluated by the relative change rate of particle size as given by Eqs. (1)–(3), respectively.

$$S_T = \left(1 - \frac{|D_0 - D_T|}{D_0} \right) \times 100\% \quad (1)$$

$$S_C = \left(1 - \frac{|D_0 - D_C|}{D_0} \right) \times 100\% \quad (2)$$

$$S_{ST} = \left(1 - \frac{|D_0 - D_{ST}|}{D_0} \right) \times 100\% \quad (3)$$

where the D₀ is the original particle size of RCCM, YCCM, and BCCM. D_T, D_C, and D_{ST} are the particle size of the samples after storing at different temperatures, in the upper of the centrifugal tube, and after storing on different days, respectively.

The monomer conversion (Conv.) of the RCCM, YCCM, and BCCM was calculated as follows:

$$\text{Conv.} = \frac{S}{S_t} \times 100\%$$

where S and S_t are the experimental solid content and theoretical solid content, respectively.

Methanol is a good solvent for the dyes; the unreacted dye can be extracted. The prepared RCCM, YCCM, and BCCM were extracted with methanol in a Soxhlet apparatus for 5 h, and the unreacted dye in the extract solution was quantified by the UV–vis absorption method. The dye conversion (Conv._{dye}) was calculated as follows:

$$\text{Conv.}_{\text{dye}} = \left(1 - \frac{Me}{M} \right) \times 100\%$$

where the Me and M are the extracted dye and the dye used in the recipe, respectively.

Results and discussion

Synthetic process and spectra properties of polymerizable dyes

Due to large electron delocalization and strong molecular copolarity, anthraquinone as a chromophore was usually used in the preparation of textile dyestuffs, which can give the excellent color brilliance and fastness of colored fabrics [24–26]. In this paper, the polymerizable dyes with three-primary colors (AHAQ, AAQCB, AHMAQ) were synthesized by introducing the C=C double bonds into the structure of anthraquinone maternal and the synthetic process was shown in Fig. S1. The chemical structure of AHAQ, AAQCB, and AHMAQ were characterized by ¹H-NMR, FT-IR, and elemental analysis, and the results are shown in Figs. S2, S3, and S4. Furthermore, the UV–vis spectra of AHAQ, AAQCB, and AHMAQ were measured to characterize the hues of synthesized polymerizable dyes using methyl alcohol as a solvent with a concentration of 1.0 × 10⁻⁴ mol/L. As shown in Fig. 1a–c, the maximum absorption wavelength (λ_{max}) of AHAQ, AAQCB, and AHMAQ exhibited at 503 nm, 406 nm, and 647 nm, indicating the red, yellow, and blue hues of dyes, respectively. The photos of dye powders were also consistent with the above results.

AMAQ: ¹H-NMR (400 MHz, CDCl₃-d₆, TMS, δ/ppm; Fig. S2a): 9.74 (s, 1H), 8.27–7.05 (m, 7H), 3.32 (s, 2H), 2.71 (s, 2H), 1.86–1.18 (m, 8H). FT-IR (KBr, cm⁻¹; Fig. S2c): 2920, 2583 (-CH₂-), 3450 (-NH-). Elemental analysis: Calc. C 74.51, H 6.88, N 8.69, O 9.92, Found: C 74.50, H 6.82, N 8.69, O 9.98.

AHAQ: ¹H-NMR (400 MHz, CDCl₃-d₆, TMS, δ/ppm; Fig. S2b): 9.75 (s, 1H), 8.25–7.05 (m, 7H), 6.28 (s, 1H), 6.06 (t, 1H), 5.62 (d, 2H), 3.36 (m, 4H), 1.87–1.20 (m, 8H). FT-IR (KBr, cm⁻¹; Fig. S2c): 2920, 2583 (-CH₂-), 3450 (-NH-),

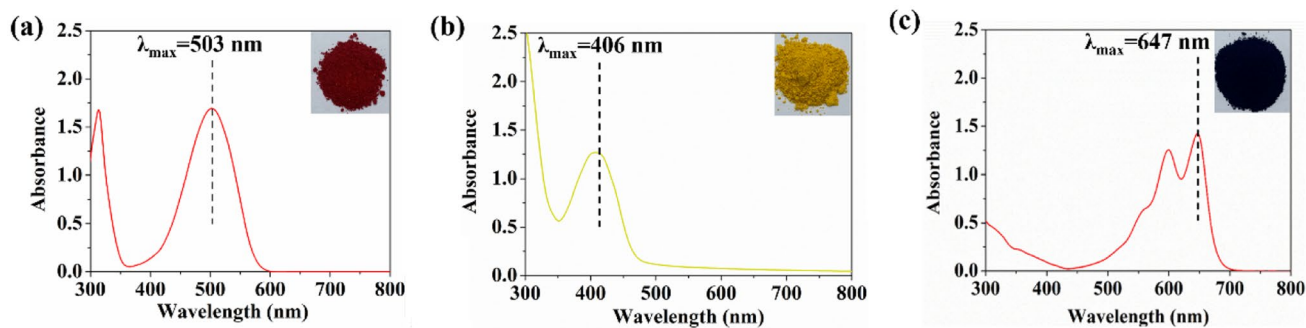


Fig. 1 UV-vis spectra of **a** AHAQ, **b** AAQCB, and **c** AHMAQ

1644 (-C=C-). Elemental analysis: Calc. C 73.38, H 6.43, N 7.44, O 12.75, Found: C 73.48, H 6.34, N 7.45, O 12.68.

AABC: ¹H-NMR (400 MHz, CDCl₃-d₆, TMS, δ/ppm; Fig. S3a): 13.50 (s, 1H), 9.35 (d, 1H), 8.39–8.27 (m, 5H), 8.18–8.15 (d, 1H), 7.91–7.83 (m, 4H). FT-IR (KBr, cm⁻¹; Fig. S3c): 1775, (-C=O). Elemental analysis: Calc. C 67.79, H 3.10, N 3.59, O 16.42, Found: C 67.74, H 3.12, N 3.56, O 16.42.

AAQCB: ¹H-NMR (400 MHz, DMSO-d₆, TMS, δ/ppm; Fig. S3b): 13.05 (s, 1H), 9.12 (d, 1H), 8.27–7.96 (m, 10H), 6.37–5.99 (m, 3H), 4.60–4.52 (d × d, 4H). FT-IR (KBr, cm⁻¹; Fig. S3c): 2920, (-CH₂-), 1775, (-C=O), 1636, (-C=C-). Elemental analysis: Calc. C 71.52, H 4.22, N 3.09, O 21.17, Found: C 71.50, N 3.09, H 4.21, O 21.16.

AHMQ: ¹H-NMR (400 MHz, CDCl₃-d₆, TMS, δ/ppm; Fig. S4a): 8.33 (m, 2H), 7.77 (m, 2H), 7.11 (m, 2H), 3.71–3.22 (m, 4H), 3.06 (s, 3H), 1.57–1.29 (m, 8H). FT-IR (KBr, cm⁻¹; Fig. S4c): 2927, 2853 (-CH₂-). Elemental analysis: Calc. C 71.77, H 7.17, N 11.96, O 9.10, Found: C 71.76, N 11.92, H 7.13, O 9.09.

AHMAQ: ¹H-NMR (400 MHz, CDCl₃-d₆, TMS, δ/ppm; Fig. S4b): 8.32 (m, 1H), 7.77 (m, 1H), 7.48 (m, 1H), 7.35 (m, 1H), 6.31 (d, 1H), 6.12 (d, 1H), 6.63 (d, 1H), 3.39 (m, 4H), 3.12 (s, 3H), 1.86–1.27 (m, 8H). FT-IR (KBr, cm⁻¹; Fig. S4c): 2927, 2853 (-CH₂-), 1648 (-C=C-). Elemental analysis: Calc. C 71.09, H 6.71, N 10.36, O 11.84, Found: C 71.03, N 10.75, H 6.71, O 11.82.

Preparation and characterization of cationic colored polymer nanospheres

In this paper, the cationic colored polymer nanospheres (RCCM, YCCM, and BCCM) were prepared by emulsion polymerization. The preparation process is shown in Fig. 2a, and their chemical structures are shown in Fig. 2b–d, respectively. St was selected as a based monomer due to its good polymerizability. The polymerizable dyes (AHAQ, AAQCB, and AHMAQ) can copolymerize with St for obtaining the different hues of prepared cationic colored polymer nanospheres.

CTE-31700 as a common commercial cationic emulsifier was used to disperse the monomers, which can also absorb onto the surface of nanospheres to provide the corresponding positive charge. The effects of polymerizable dyes on monomer conversion (Conv.) and dye conversion (Conv._{dye}) are shown in Table S1. Conv._{dye} is a crucial factor for determining the color strength of RCCM, BCCM, and YCCM. It can be seen that the Conv._{dye} of RCCM, BCCM, and YCCM decreased with the increase of AHAQ, AAQCB, and AHMAQ contents. This phenomenon can be explained by the slower diffusion of the water-insoluble polymerizable dyes from the monomers into the growing particles through the aqueous phase. Furthermore, the dyes would precipitate as dyestuff aggregates if a large amount of dye was employed in the recipe, resulting in a lower dye conversion [27, 28]. Then the monomer conversion was also studied and the results are also shown in Table S1. Although the dye conversion decreased with the increase of dye contents, the total monomer conversion changed slightly with the increase of dye contents.

The size distribution and morphologies (Fig. 3a–c) of prepared RCCM, YCCM, and BCCM were measured by DLS and TEM. It can be seen that the RCCM, YCCM, and BCCM exhibited a regular monodispersed spherical shape with average diameters of 65 nm, 68 nm, and 69 nm, respectively. Dispersion stability is an important index for evaluating the dispersibility of RCCM, YCCM, and BCCM. Hence, the thermal stability (S_T), centrifugal stability (S_C), and storage stability (S_{ST}) of RCCM, YCCM, and BCCM were measured and the results are shown in Fig. 2d–f. In the testing of thermal stability, the particle size of RCCM, YCCM, and BCCM decreased by 9.90%, 8.47%, and 8.14% at 90 °C for 72 h, respectively. In the testing of centrifugal stability, the particle size of RCCM, YCCM, and BCCM decreased by 7.49%, 6.79%, and 6.75% at 5000 rpm for 30 min, respectively. The particle size decreased by 11.75%, 9.75%, and 9.57% of RCCM, YCCM, and BCCM after storing for 30 days. The above results indicated that the RCCM, YCCM, and BCCM exhibited excellent dispersion stability.

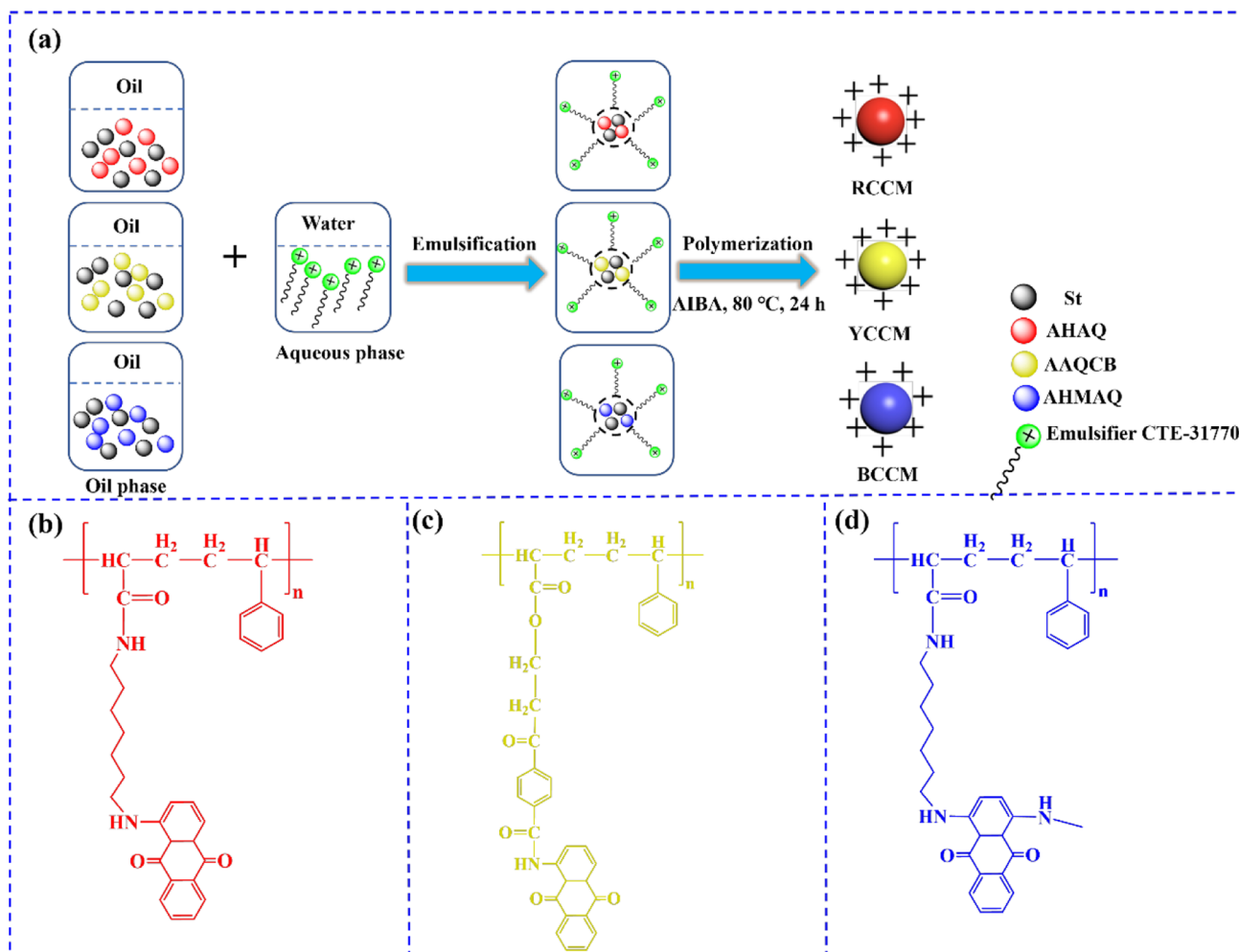


Fig. 2 a Preparation process of RCCM, YCCM, and BCCM; chemical structure of **b** RCCM, **c** YCCM, and **d** BCCM

Meanwhile, the zeta potentials of RCCM, YCCM, and BCCM were +42.8 mV, +45.3 mV, and +50.6 mV, which can be attributed to the enrichment of cationic emulsifier (CTE-31700) on the surface of nanospheres. Furthermore, the high zeta potential also ensured the high dispersion stability of RCCM, YCCM, and BCCM [27]. However, the thermal, centrifugal, and storage stability of RCCM were slightly lower than those of YCCM, and BCCM, which was attributed to the lower zeta potential of YCCM as compared with YCCM, and BCCM.

The DTG curves of AHAQ, AAQCB, AHMAQ, RCCM, YCCM, and BCCM were measured, and results are shown in Fig. 4a–f. For AHAQ (Fig. 4a), AAQCB (Fig. 4c), and AHMAQ (Fig. 4e), the weight losses occurred at 364.25 °C, 217.15 °C, and 329.78 °C due to the thermal decomposition of carbon–carbon double bonds ($-C=C-$) [29]. The weight losses at the stage of 445.48 °C, 430.09 °C, and 428.71 °C were due to the decomposition of aromatic rings

[30]. Additionally, for AHMAQ, a weight loss at a stage of 123.08 °C was due to the loss of absorbed water [31]. For RCCM, YCCM, and BCCM, similar DTG curves can be observed in Fig. 4b, d, f. At the stage of 275.55 °C, 290.90 °C, and 282.76 °C, about 10.10%, 13.87%, and 9.98% weight losses occurred, resulting from the decomposition of polymerizable dyes. Meanwhile, the 88.65%, 86.04%, and 89.95% weight losses at the stage of 447.48 °C, 445.07 °C, and 446.02 °C were caused by the thermal decomposition of the polymer structure [29]. DSC measurement is an effective approach to study the glass transition temperature (T_g) and physical changes of polymers. DSC curves of RCCM, YCCM, and BCCM appeared in Fig. 4g. All of the samples exhibited two T_g s. The T_g at 54 °C was attributed to the copolymers enriched with polymerizable dyes and the T_g at 101 °C presumably due to the St homopolymer moiety. This discontinuity might be an indication of the microphase separation of dyes and St components because of their

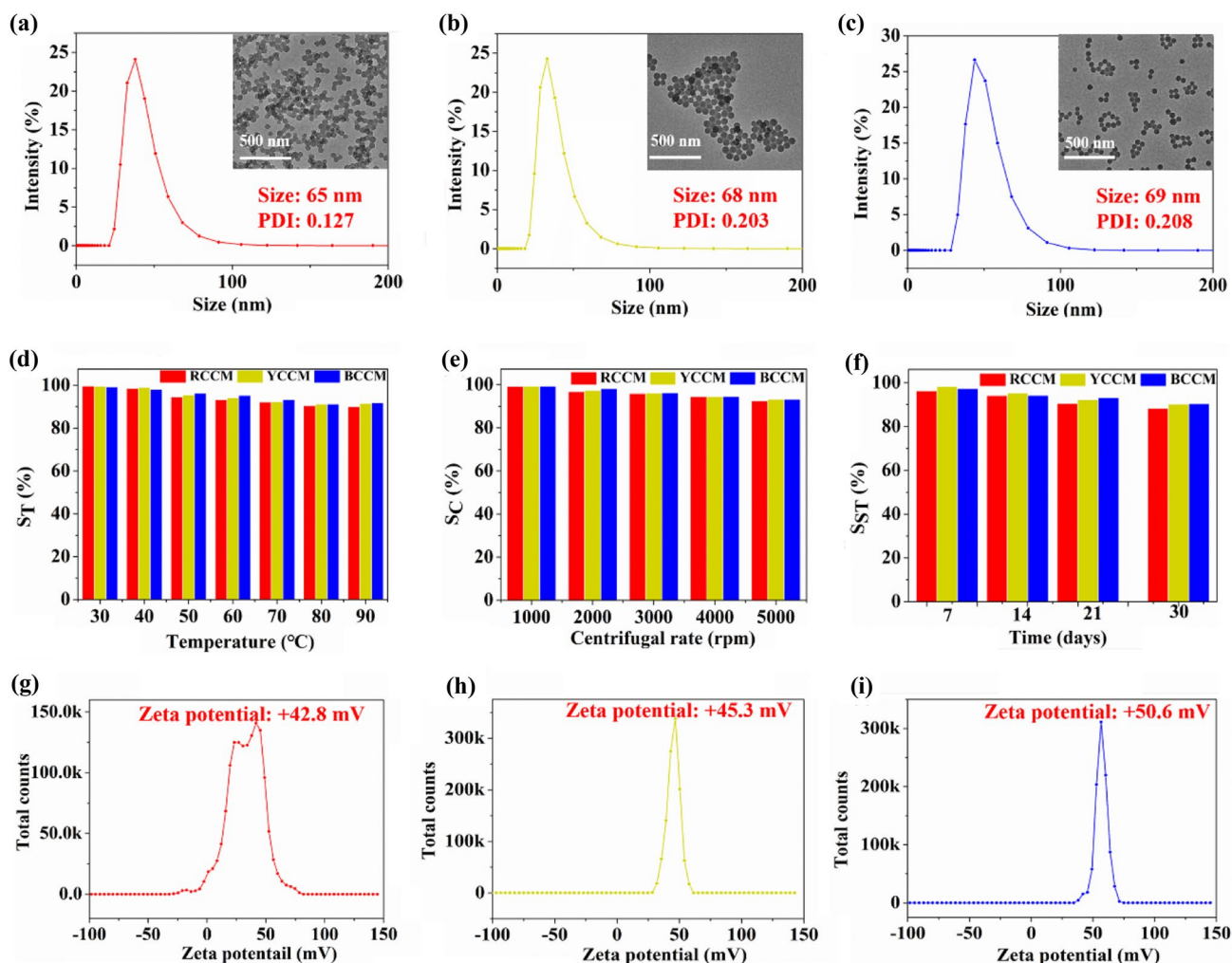


Fig. 3 TEM images and particle size of **a** RCCM, **b** YCCM, and **c** BCCM, **d** thermal, **e** centrifugal, and **f** storage stability of RCCM, YCCM, and BCCM; zeta potential of **g** RCCM, **h** YCCM, and **i** BCCM

incompatibilities [32, 33]. The prepared RCCM, YCCM, and BCCM were characterized by FT-IR, and results are shown in Fig. 4h. Because of the low amount of polymerizable dyes (about 1.5 wt% with respect to the total amount of St), the resulted FT-IR spectra did not display significant differences for all the samples. The peaks at 2920 cm^{-1} and 2850 cm^{-1} were assigned to stretching vibration of $-\text{CH}_2-$ groups in polymerizable dyes and St, and the peaks at 1680 cm^{-1} were assigned to carbonyl groups ($\nu_{\text{C=O}}$) of polymerizable dyes. The XRD patterns of AHAQ, AAQCB, AHMAQ, RCCM, YCCM, and BCCM were compared in Fig. 4i. It can be seen that XRD patterns of RCCM, YCCM, and BCCM were similar and the characteristic diffraction peaks appeared about in $2\theta = 10^\circ$ and 19° . However, the characteristic peaks of AHAQ, AAQCB, and AHMAQ were

not observed in RCCM, YCCM, and BCCM curves, indicating that the dyes had been involved in the copolymerization and it exited as monomolecular into polymer chains [34].

As seen in Fig. 5, λ_{max} of polymerizable dyes and prepared polymer nanospheres exhibited at 503 nm, 406 nm, and 607 nm, respectively. No significant bathochromic or hypsochromic shifts of λ_{max} were observed between the polymerizable dyes and prepared polymer nanospheres, indicating that the anthraquinone chromophores did not change before and after the copolymerization. Also, it can be concluded that the anthraquinone chromophores were distributed uniformly on the polymer chain; both the dye aggregation and the π - π stacking interaction were excluded from the results, since those would generate the bathochromic shift of λ_{max} [35, 36].

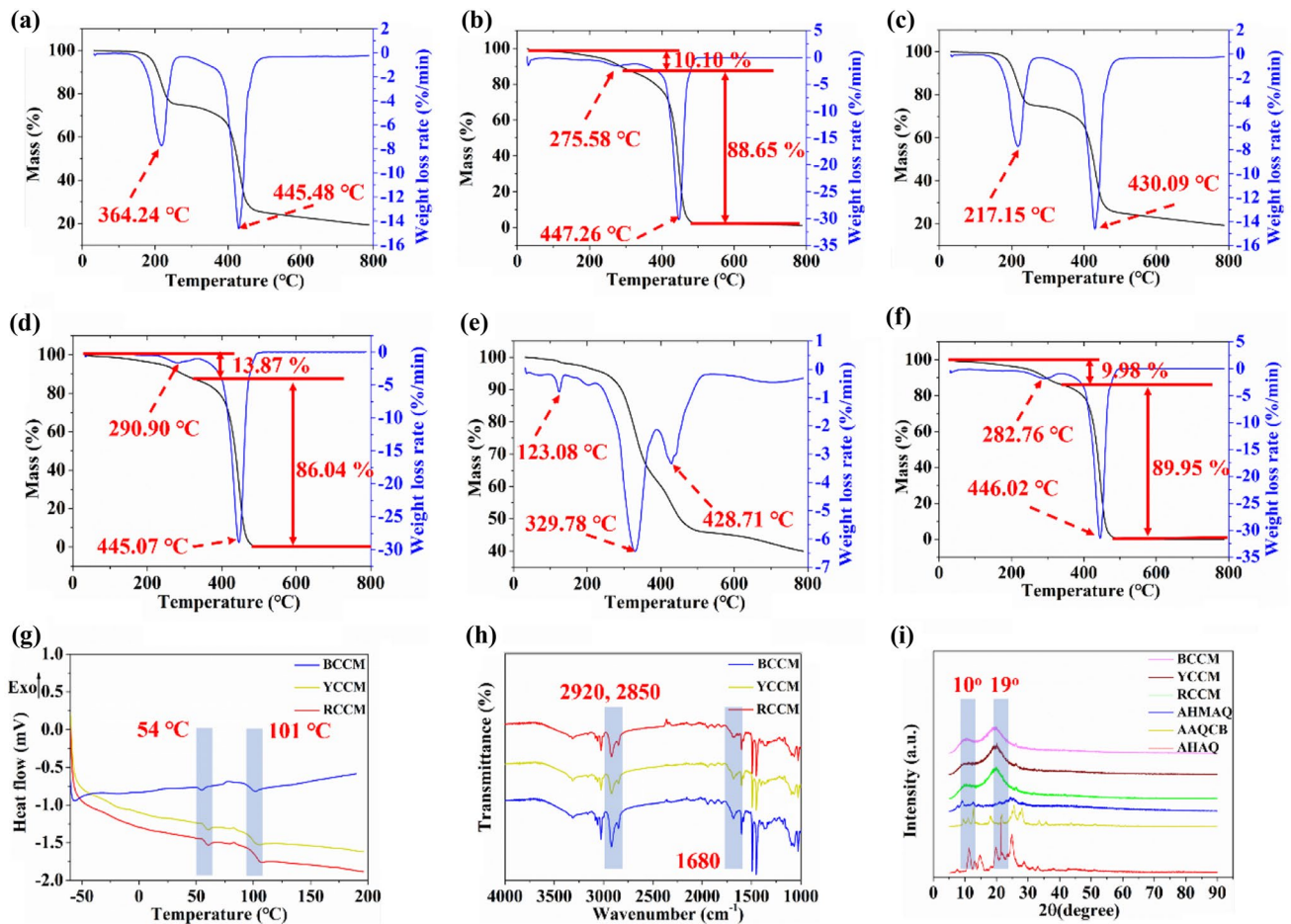


Fig. 4 TG and DTG curves of **a** AHAQ, **b** RCCM, **c** AAQCB, **d** YCCM, **e** AHMAQ, and **f** BCCM; DSC curves of RCCM, YCCM, and BCCM; FT-IR spectra of RCCM, YCCM, and BCCM; and XRD patterns of AHAQ, AAQCB, AHMAQ, RCCM, YCCM, and BCCM

Preparation and properties of printed cotton fabric

To obtain more negative charges and enhance the absorption capacity for cationic compounds, the cotton fabrics were modified by CMC. The process of treatment has

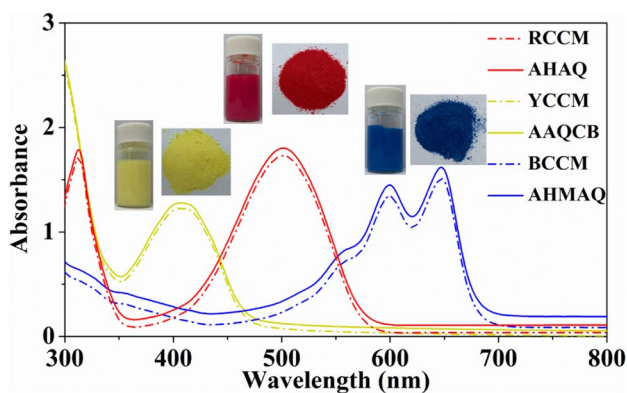
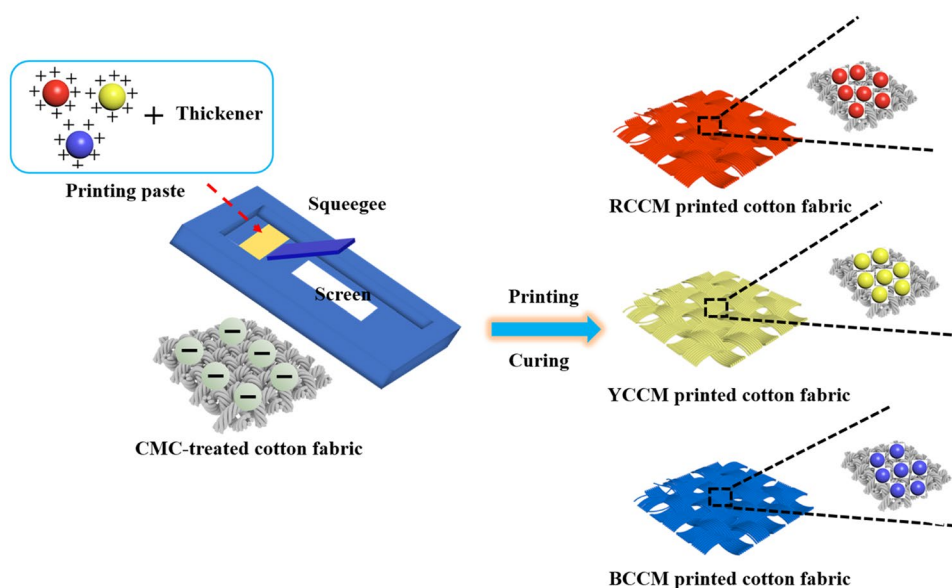


Fig. 5 UV-vis spectra of AHAQ, AAQCB, AHMAQ, RCCM, YCCM, and BCCM

been reported [22]. As seen in Fig. 6, the prepared RCCM, YCCM, and BCCM were absorbed onto the surface of CMC-treated cotton fabrics through the electrostatic attraction between the anionic fabrics and cationic nanospheres after screen printing. The effects of curing temperature and time on the color strength (K/S value) of RCCM, YCCM, and BCCM printed fabrics were studied in Fig. S5. It can be seen that the K/S values of printed cotton fabrics increased with the increase of curing temperature and reached a maximum K/S value at 150 °C (Fig. S5a). Figure S5b shows that the absorption time had an obvious effect on the K/S value, which reached a maximum value after 150 s.

In general, cotton fibers are prone to absorb a significant amount of water because they have a large number of hydroxyl groups in their structure [37]. In Fig. 7a, the wettability of the cotton fabrics and printed cotton fabrics was studied by measuring the static water contact angle (CA). Compared with cotton fabric, the CA of RCCM printed fabric, YCCM printed fabric, and BCCM printed fabric were 127°, 128°, and 123°. This phenomenon can be




Fig. 6 The printing process of RCCM, YCCM, and BCCM

explained that the RCCM, YCCM, and BCCM on the surface of cotton fabric resulted in the rough surface of printed fabrics (Fig. 7c–e) as compared with the smooth surface of unprinted fabrics (Fig. 7b) [38]. The color parameters (L^* , a^* , b^*), color strength (K/S value), and color difference (ΔE) were summarized in Table 3. L^* refers to brightness–darkness with values from 100 to 0 representing white to black. a^* is the red–green coordinate axis, and the positive direction is red, and the negative direction is green. b^* is the yellow–blue coordinate axis, and the positive direction is yellow, and the negative direction is blue. The K/S value and ΔE represent the surface color strength and color uniformity of colored samples, respectively. As seen in Table 3, the results showed that the printed fabrics exhibited the hues of red, yellow, and blue with the K/S values of 4.25, 3.95, and 3.02, respectively. The lower the values of ΔE , the higher the uniformly the colored samples. In Table 3,

the lower values of ΔE indicated that the uniform color of RCCM, YCCM, and BCCM printed fabrics. Meanwhile, the photos of printed fabrics also proved the better color performance and pattern fineness of RCCM, YCCM, and BCCM printed fabrics.

The hand feel and color fastness of printed fabrics were measured and the results are shown in Table 4. Compared with cotton fabrics, the resilience score, softness score, and smoothness score of RCCM, YCCM, and BCCM printed fabrics were changed slightly. Additionally, the values of relative hand feel also indicated that the hand feel of printed samples had no significant changes. The color fastness was also studied, and results showed that the printed fabrics exhibited a good change in rubbing fastness (4 and 3–4 grade) and washing fastness (3–4 and 4 grade), which can be attributed that ionic bonds between the anionic cotton fabrics and cationic polymer nanospheres.

Table 3 Color parameters of printed fabrics

Samples	L^*	a^*	b^*	K/S value	ΔE	
RCCM printed fabric	52.24	52.92	10.33	4.25	0.12	
YCCM printed fabric	88.83	-2.97	53.35	3.95	0.15	
BCCM printed fabric	52.98	-5.48	-26.66	3.02	0.18	

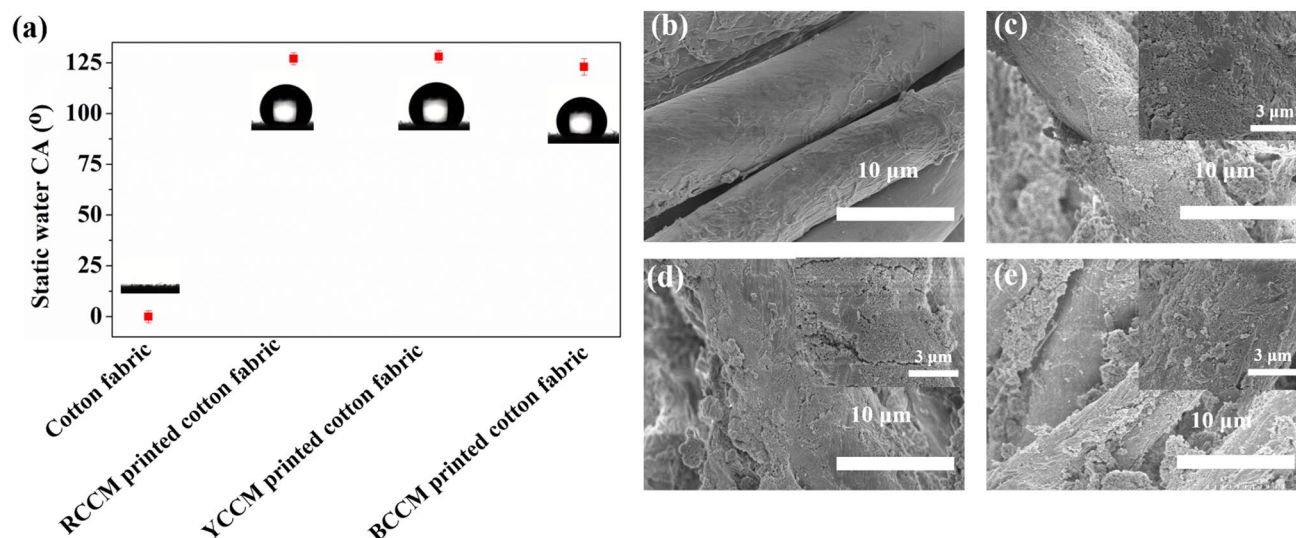


Fig. 7 a Hydrophobicity of samples and SEM images of **b** cotton fabric, **c** RCCM printed fabrics, **d** YCCM printed fabric, and **e** BCCM printed fabrics

Table 4 Hand feel and fastness of the printed fabrics

Properties		Cotton fabric	RCCM printed fabric	YCCM printed fabric	BCCM printed fabric
Resilience score		30.48	32.05	33.19	32.85
Softness score		90.53	85.23	82.06	88.23
Smoothness score		88.68	90.25	91.15	90.28
Relative hand feel		—	3.45	3.08	2.97
Rubbing fastness	Dry	—	4	4	4
	Wet	—	3–4	3–4	3–4
Wetting fastness	Changing	—	3–4	3–4	3–4
	Staining	—	4	4	4

Conclusions

In this paper, we aimed at the preparation of colored cotton fabrics by cationic colored polymer nanospheres. The polymerizable dyes (AHAQ, AAQBC, and AHMAQ) were successfully synthesized and used together with St as the monomers to prepare the monodispersed cationic colored polymer nanospheres (RCCM, YCCM, and BCCM) via emulsion polymerization. RCCM, YCCM, and BCCM presented the monodispersed spherical distribution with diameters of 65 nm, 68 nm, 69 nm, and zeta potentials of +42.8 mV, +45.3 mV, and +50.6 mV. The positive charges of nanospheres surface provided the preferable dispersion stability of nanospheres dispersion system. The nanospheres were used to print CMC-treated cotton fabrics by electrostatic forces. The nanospheres printed fabrics exhibited a certain hydrophobicity with the contact angles of 127°, 128°, and 123°, and a similar hand feel as compared with printed fabrics. The color fastness of nanospheres printed fabrics were 4, 3–4, 3–4, and 4 grades,

showing good color fastness for practical applications. This work provides a strategy for the preparation of novel colorants for textile coloration.

Supplementary information The online version contains supplementary material available at <https://doi.org/10.1007/s00396-021-04855-0>.

Funding This work was supported by the Natural Science Foundation of Jiangsu Province (grant number BK20191334).

Declarations

Conflict of interest The authors declare no competing interests.

References

- Dong X, Gu Z, Hang C, Ke G, He J (2019) Study on the salt-free low-alkaline reactive cotton dyeing in high concentration of ethanol in volume. *J Clean Prod* 226:316–323

2. Rosa JM, Fileti AMF, Tambourgi EB, Santana JCC (2015) Dyeing of cotton with reactive dyestuffs: the continuous reuse of textile wastewater effluent treated by Ultraviolet/Hydrogen peroxide homogeneous photocatalysis. *J Clean Prod* 90:60–65
3. Fang L, Zhang X, Sun D (2013) Chemical modification of cotton fabrics for improving utilization of reactive dyes. *Carbohydr Polym* 91:363–369
4. A JO, A JM, A FW, A WL, A XF, A SL, B AA (2020) Unexpected superhydrophobic polydopamine on cotton fabric. *Prog Org Coat* 147
5. Elhalawany N, ME El-Naggar, A Elsayed, AR Wassel, MAA Elghaffar (2020) Polyaniline/zinc/aluminum nanocomposites for multifunctional smart cotton fabrics. *Mater Chem Phys* 249: 123210
6. Nallathambi A, Venkateswarapuram Rengaswami GD (2017) Industrial scale salt-free reactive dyeing of cationized cotton fabric with different reactive dye chemistry. *Carbohydr Polym* 174:137–145
7. Arivithamani N, Dev VRG (2018) Characterization and comparison of salt-free reactive dyed cationized cotton hosiery fabrics with that of conventional dyed cotton fabrics. *J Clean Prod* 183:579–589
8. Salimpour A, Malek RA, Mazaheri F (2015) Salt-free dyeing isotherms of cotton fabric grafted with PPI dendrimers. *Cellulose* 22:897–910
9. Mu B, Liu L, Li W, Yang Y (2019) High sorption of reactive dyes onto cotton controlled by chemical potential gradient for reduction of dyeing effluents. *J Environ Manage* 239:271–278
10. Jiang X, Cai K, Zhang J, Shen Y, Wang S, Tian X (2011) Synthesis of a novel water-soluble chitosan derivative for flocculated decolorization. *J Hazard Mater* 185:1482–1488
11. Aksu Z, Doenmez G (2005) Combined effects of molasses sucrose and reactive dye on the growth and dye bioaccumulation properties of *Candida tropicalis*. *Process Biochem* 40:2443–2454
12. Mohsin M, Sardar S (2019) Multi-criteria decision analysis for textile pad-dyeing and foam-dyeing based on cost, performance, productivity and sustainability. *Cellulose* 26:4143–4157
13. Vishnu G, Kurian J (2008) Decolorization of reactive dyebath containing high exhaust and low salt dyes by nanofiltration and its reuse. *Environ Prog* 27:30–39
14. Ramalingam S, Sreeram KJ, Raghava Rao J, Unni Nair B (2016) Organic nanocolorants: self-fixed, optothermal resistive, silica-supported dyes for sustainable dyeing of leather. *ACS Sustain Chem Eng* 4:2706–2714
15. Yin P, Wu G, Qin W, Chen X, Chen H (2012) CYM and RGB colored electronic inks based on silica-coated organic pigments for full-color electrophoretic displays. *J Mater Chem C* 1:843–849
16. Han ZW, Wang Z, Feng XM, Li B, Mu ZZ, Zhang JQ, Niu SC, Ren LQ (2106) Antireflective surface inspired from biology: a review. *Biosurface Biotribology* 2:137–150
17. Li Y, Zhang J, Yang B (2010) Antireflective surfaces based on biomimetic nanopillared arrays. *Nano Today* 5:117–127
18. Song Y, Fang K, Ren Y, Tang Z, Wang R, Chen W, Xie R, Shi Z, Hao L (2018) Inkjet printable and self-curable disperse dyes/P(St-BA-MAA) Nanosphere Inks for Both Hydrophilic and Hydrophobic Fabrics. *Polymers* 10:2073–4360
19. Fang K, Ren B (2014) A facile method for preparing colored nanospheres of poly(styrene-co-acrylic acid). *Dyes Pigments* 100:50–56
20. Fang K, Xie R, Liu X, Zhao G, Han D, Chen W, Shi Z, Hao L, Cai Y (2016) Reactive dye/poly(styrene-co-butyl acrylate-co-trimethyl(vinylbenzyl) ammonium chloride) nanospheres with high coloration performance for cleaner dyeing of cotton fabrics. *Cellulose* 26:5807–5819
21. Yang Y, Li M, Fu S (2021) Use of highly-stable and covalently bonded polymer colorant on binder-free pigment printing of citric acid treated cotton fabric. *Cellulose* 28:1843–1856
22. Liu D, Hao L, Fang K (2014) Adsorption of cationic copolymer nanospheres onto cotton fibers investigated by a facile nephelometry. *Colloid Surface A* 452:82–88
23. Fras-Zemljič L, Stenius P, Laine J, Stana-Kleinschek K (2006) The effect of adsorbed carboxymethyl cellulose on the cotton fibre adsorption capacity for surfactant. *Cellulose* 13:655–663
24. Fu S, Lu J, Luo X, Bai F (2013) Preparation of disperse dye/latex dispersion for printing of cellulose fabric. *Colloid Surface A* 423:131–138
25. Fu S, Zhang G, Du C, Tian A (2012) Preparation of encapsulated disperse dye dispersion for polyester inkjet printing ink. *J Appl Polym Sci* 121:1616–1621
26. Yang Y, Li M, Tang A, Liu Y, Li Z, Fu S (2020) Preparation of Covalent and solvent-resistance colored latex particles and its application on cotton fabric. *Fibers Polymers* 21:1685–1693
27. Ruckerova A, Machotova J, Svoboda R, Pukova K, Bohacik P, Valka R (2018) Ambient temperature self-crosslinking lattices using low generation PAMAM dendrimers as inter-particle crosslinking agents. *Prog Org Coat* 119:91–98
28. Me A, Rs B, Mg A (2016) Development of self-curable hybrid pigment inks by miniemulsion polymerization for inkjet printing of cotton fabrics. *Dyes Pigments* 133:467–478
29. Song Y, Fang K, Bukhari MN, Ren Y, Zhang K, Tang Z (2020) Green and efficient inkjet printing of cotton fabrics using reactive dye@copolymer nanospheres. *ACS Appl Mater Interfaces* 12:45281–45295
30. Gonul Y, Felgueiras HP, Isabel RA, Necdet S, Andrea Z, Pedro SA (2018) Dyed poly(styrene-methyl methacrylate-acrylic acid) photonic nanocrystals for enhanced structural color. *ACS Appl Mater Interfaces* 10:23285–23294
31. Hao L, Fang K, Wang R, Cai Y (2017) The modification of cotton substrate using chitosan for improving its dyeability towards anionic microencapsulated nano-pigment particles. *Ind Crop Prod* 95:348–356
32. LüT QD, Zhang D, Liu Q, Zhao H (2016) Fabrication of self-cross-linking fluorinated polyacrylate latex particles with core-shell structure and film properties. *React Funct Polym* 104:9–14
33. Adelnia H, Nasrollah Gavgani J, Riazi H, Cheraghi Bidsorkhi H (2014) Transition behavior, surface characteristics and film formation of functionalized poly(methyl methacrylate-co-butyl acrylate) particles. *Prog Org Coat* 77:1826–1833
34. Ding L, Jiang Y, Wang B, Li Y, Mao Z, Xu H, Zhong Y, Zhang L, Sui X (2018) A waterborne bio-based polymer pigment: colored regenerated cellulose suspension from waste cotton fabrics. *Cellulose* 25:7369–7379
35. Li B, Shen J, Liang R, Ji W, Kan C (2012) Synthesis and characterization of covalently colored polymer latex based on new polymerizable anthraquinone dyes. *Colloid Polym Sci* 290:1893–1900
36. Li B, Shen J, Jiang Y, Wang J, Kan C (2013) Preparation and properties of covalently colored polymer latex based on a new anthraquinone monomer. *J Appl Polym Sci* 129:1484–1490
37. Nabipour H, Wang X, Song L, Hu YJC (2020) Hydrophobic and flame-retardant finishing of cotton fabrics for water–oil separation. *Cellulose* 27:4145–4159
38. Liu J, Dong C, Zhang Z, Kong D, Sun H, Lu ZJC (2020) Multifunctional flame-retarded and hydrophobic cotton fabrics modified with a cyclic phosphorus/polysiloxane copolymer. *Cellulose* 27:3531–3549

Publisher's Note Springer Nature remains neutral with regard to jurisdictional claims in published maps and institutional affiliations.